

Consideration of local stiffening and clearance nonlinearities in coupled systems using a generalized Harmonic Balance Method

S. Peter, F. Schreyer, P. Reuss, L. Gaul

University of Stuttgart, Institute of Applied and Experimental Mechanics,

Pfaffenwaldring 9, 70569 Stuttgart, Germany

email: {peter,schreyer,reuss,gaul}@iam.uni-stuttgart.de

Abstract

In many assembled structures local nonlinearities can be found, which affect the overall dynamics of the system. Typical examples are joints which show nonlinear behavior due to friction as well as clearance. Another example are bushing elements which are used as connectors in the automotive industry, showing a stiffening effect and frequency dependence. In both examples it is of interest to model the effect of such local nonlinearities on the dynamics of large scale finite element (FE) assemblies in the context of substructuring. In this contribution a clearance nonlinearity is considered leading to a non-smooth, nonlinear force resulting in similar dynamics like in classical vibro-impact-systems. In contrast, the bushing elements can be modeled by a smooth nonlinear function characterizing a progressive spring behavior. Nevertheless, in both cases similar nonlinear phenomena like the occurrence of predominantly subharmonic solutions and strong influence of higher harmonics can be observed. Thus, Frequency Response Functions (FRFs) are calculated using a generalized Harmonic Balance Method (HBM) taking these effects into account. For both nonlinearities the resonance peaks are bent towards higher frequencies with increasing amplitude, resulting in a frequency range with multiple solutions. Also, the existence of predominantly subharmonic solutions results in additional bends in the FRFs. To be able to capture the existence of multiple, stable and unstable solutions at certain frequencies a Predictor-Corrector continuation method is used for the calculation of the solutions. Additionally, the dependence of the backbone curve on the amplitude or the total energy in the system respectively, is visualized in Frequency Energy Plots (FEPs). Furthermore, the corresponding Non-linear Normal Modes (NNM) are depicted. In these plots also the effect of modal interactions, like energy transfer between modes can be shown. To demonstrate the proposed method a four mass oscillator is used. This oscillator consists of two linear substructures which are coupled by the nonlinear elements. However, the methods can be easily extended to FE models with local nonlinearities or used in the context of substructuring. The methods are used for further investigations of beam structures including such nonlinearities and will be validated by experimental data.

1 Introduction

Local nonlinearities can have strong influence on the vibrations of assembled structures. Therefore, it is crucial to take these nonlinearities into account when simulating the behavior of such systems. In this paper a method for efficient calculation of assembled structures with local nonlinearities is proposed. For these calculations a generalized version of the Harmonic Balance Method, taking into account higher harmonic as well as subharmonic responses, is used. This method can be combined with dynamic substructuring and reduction methods, like the Frequency Based Substructuring (FBS) method [1] or Component Mode Synthesis (CMS) [2, 4], to be able to calculate large scale finite element models. In this context the local nonlinearities

can be regarded as nonlinear coupling elements like it is shown in Fig. 1.

In the following, two different nonlinearities are considered. The first one represents clearance in assembled structures and the second one a nonlinear bushing element showing stiffening behavior. The nonlinearities are described in detail in Section 2. As both nonlinearities discussed in this paper are of the stiffening type, which causes resonance peaks to bend towards higher frequencies with growing amplitude, frequency ranges with multiple solutions occur. To capture these multiple solutions, the HBM is combined with a continuation method [3]. As a part of the solution algorithm, a purely analytical approach for the computation of the nonlinear forces and the Jacobian matrix of the system is presented, resulting in very fast and robust calculations. This solution method is described in detail in Section 3 for the calculation of Frequency Response Functions (FRF). Some features of the systems regarded in this paper, like the frequency energy dependence or modal interactions, can be visualized and explained by Nonlinear Normal Modes (NNM) and Frequency Energy Plots (FEP) [5, 6]. Section 4 briefly mentions some aspects of the NNM and FEP calculations based on the HBM. The proposed methods are demonstrated on a four mass oscillator in Section 5. The paper closes in Section 6 with a conclusion and suggestions for future research.

2 System representation and types of nonlinearity

In this Section, the system to which this paper refers to is described. Therefore, firstly a substructure formulation is briefly reviewed and the coupling is explained. For the sake of brevity the coupling is sketched in the physical domain only, however it can be performed analogous in the frequency domain using an FBS formulation [1] or it can be combined with model reduction techniques yielding a CMS formulation [2, 4]. The equation of motion for a general mechanical system consisting of different substructures can be written in the physical domain according to [7] as

$$\mathbf{M}\ddot{\mathbf{x}} + \mathbf{D}\dot{\mathbf{x}} + \mathbf{K}\mathbf{x} = \mathbf{f} + \mathbf{g} \quad (1)$$

where \mathbf{M} , \mathbf{D} and \mathbf{K} contain the mass, damping and stiffness matrices of all substructures in a block-diagonal form. The vector of external forces ,e.g. excitation forces, is denoted by \mathbf{f} and the vector of connecting forces between the substructures by \mathbf{g} . In the interfaces between the substructures the force equilibrium can be written as

$$\mathbf{L}^T \mathbf{g} = \mathbf{0}, \quad (2)$$

where \mathbf{L} is a Boolean matrix localizing the interface DOFs within the set of global DOFs. Introducing a Boolean matrix $\mathbf{B}^T = \text{null}(\mathbf{L}^T)$ the interface forces can be expressed using Lagrange multipliers $\boldsymbol{\lambda}$ yielding

$$\mathbf{g} = -\mathbf{B}^T \boldsymbol{\lambda}. \quad (3)$$

In this equation $\boldsymbol{\lambda}$ represents the interface forces which can be expressed as a function of the relative displacement \mathbf{u} in the interface as

$$\boldsymbol{\lambda} = \mathbf{F}_{\text{nl}}(\mathbf{u}, \dot{\mathbf{u}}) \quad (4)$$

which is related to \mathbf{x} by the Boolean matrix \mathbf{B} as

$$\mathbf{u} = \mathbf{B}\mathbf{x}. \quad (5)$$

Within this contribution nonlinear coupling elements are considered leading to coupling forces related to \mathbf{u} in a nonlinear way. Therefore the Harmonic Balance Method is utilized to approximate the nonlinear interface forces. For simplicity in the following only one DOF of both substructures is coupled with a nonlinear element reducing \mathbf{u} to a scalar quantity.

Before the HBM is explained, the two different local nonlinearities connecting linear substructures are characterized. On the one hand clearance in joints of assembled structures is represented by a piecewise linear function and on the other hand a nonlinear bushing element of an automotive brake assembly is modeled as cubic nonlinearity of the stiffening type. Both systems are depicted schematically in Fig. 1, where the linear

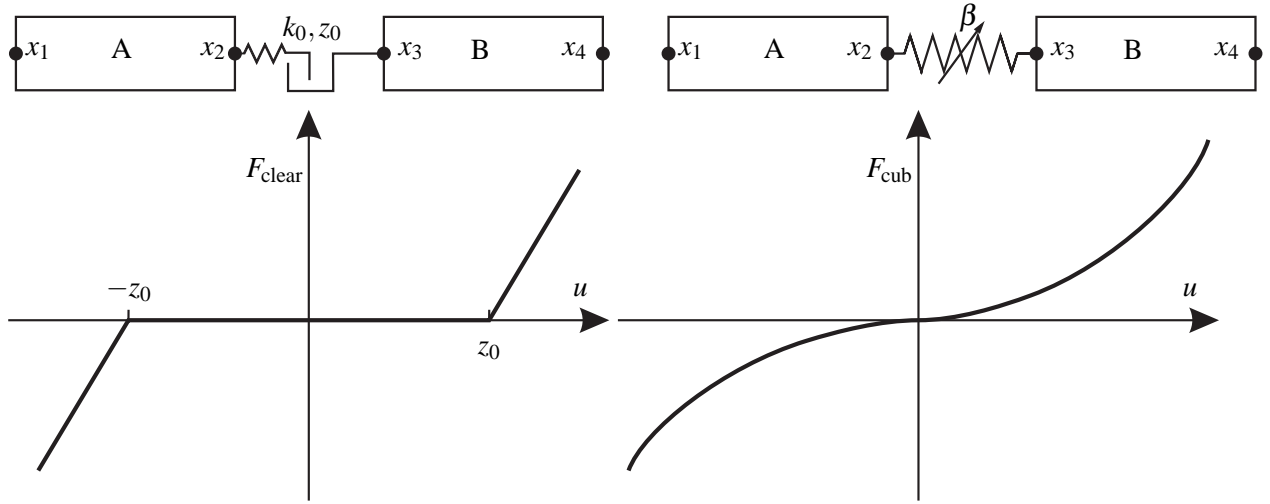


Figure 1: Schematic system representation and nonlinear forces: clearance nonlinearity (left) and cubic nonlinearity (right)

parts of the assembly are represented by the substructures A and B.

Fig. 1 also displays the nonlinear forces due to clearance F_{clear} and a cubic nonlinearity F_{cub} , which depend on the relative displacement in the coupling interface $u = x_2 - x_3$. Hence, the nonlinear force caused by the clearance can be calculated depending on u yielding a piecewise defined function

$$F_{clear} = \begin{cases} k_0(u - z_0) & u \leq -z_0 \\ 0 & -z_0 < u < z_0 \\ -k_0(u - z_0) & u \geq z_0, \end{cases} \quad (6)$$

where k_0 is the contact stiffness in the interface, which has to be taken into account when the relative displacement is larger than the clearance $\pm z_0$.

In the case of the nonlinear bushing element the force in the interface is approximated as a cubic nonlinearity with the cubic spring constant β and can be calculated by

$$F_{cub} = \beta u^3 \quad (7)$$

which also depends on the relative displacement u in a nonlinear way.

3 Harmonic Balance Method for sub- and higher harmonic response

The HBM is a method to approximately compute the steady state response of nonlinear systems [8, 9]. The method is based on the assumption that every nonlinear steady state response of a system which is driven by an excitation frequency ω can be expressed by a Fourier series with an infinite number of harmonics of this frequency. In its original version only the fundamental response is considered such that the method represents a rough approximation. For a consideration of a higher and subharmonic response like it is done in this contribution the underlying ansatz must be extended to

$$\mathbf{x}(t) = \mathbf{a}_0 + \sum_{\nu=1}^{\infty} \sum_{\mu=1}^{\infty} \mathbf{a}_{\nu/\mu} \cos\left(\frac{\nu}{\mu} \omega t\right) + \mathbf{b}_{\nu/\mu} \sin\left(\frac{\nu}{\mu} \omega t\right). \quad (8)$$

This ansatz now takes higher harmonics into account for $\nu > 1$ and subharmonics are represented by $\mu > 1$. The constant part \mathbf{a}_0 considers the mean position of the vibration. Note, that with this ansatz only harmonics

in a rational condition are respected. Linear combinations of the harmonics to represent combination resonances [10] are not considered here since the excitation for the presented system is excited with only one frequency. Using this ansatz for the calculation of the response from Eq. (8) the nonlinear forces $F_{nl}(\dot{u}, u, t)$ in Eq. (6) and (7) can be developed in a Fourier series dependent on the relative displacement u in the coupling interface which is related to \mathbf{x} by equation (5) leading to

$$F_{nl}(\dot{u}, u, t) = A_0 + \sum_{v=1}^{\infty} \sum_{\mu=1}^{\infty} A_{v/\mu} \cos\left(\frac{v}{\mu} \omega t\right) + B_{v/\mu} \sin\left(\frac{v}{\mu} \omega t\right). \quad (9)$$

This Fourier series as well as the ansatz in Eq. (8) is truncated to a finite number of harmonics N including all harmonics v_h and subharmonics μ_h , whose numbers have to be chosen depending on the kind of nonlinearity and the desired precision of the calculation. The Fourier coefficients of Eq. (9) can be written as a vector

$$\hat{\mathbf{F}}_{nl,rel} = [A_0, A_1, A_{1/2}, \dots, A_{1/\mu_h}, \dots, A_{v_h/\mu_h}, B_1, B_{1/2}, \dots, B_{1/\mu_h}, \dots, B_{v_h/\mu_h}]^T, \quad (10)$$

which can be determined via integration of

$$\hat{\mathbf{F}}_{nl,rel} = \frac{2}{\mu_h T} \int_0^{\mu_h T} \mathbf{\Gamma}_+ F_{nl}(\dot{u}, u, t) dt, \quad (11)$$

with

$$\mathbf{\Gamma}_+ = \left[\frac{1}{2}, \cos(\omega t), \cos\left(\frac{1}{2} \omega t\right), \dots, \cos\left(\frac{1}{\mu_h} \omega t\right), \dots, \cos\left(\frac{v_h}{\mu_h} \omega t\right), \sin(\omega t), \sin\left(\frac{1}{2} \omega t\right), \dots, \sin\left(\frac{1}{\mu_h} \omega t\right), \dots, \sin\left(\frac{v_h}{\mu_h} \omega t\right) \right]^T. \quad (12)$$

For the calculation of these coefficients, the regarded period length $T=2\pi/\omega$ has to have at least the length of one full period, also for the subharmonic terms which have μ_h -times the period length of the excitation. The vector of the nonlinear force $\hat{\mathbf{F}}_{nl,rel}$ depends on the relative displacement and can be localized in the global set of DOFs analogous to Eq. (5) yielding a generalized vector of nonlinear forces $\hat{\mathbf{f}}_{nl}(\hat{\mathbf{x}}, \omega)$. Assuming harmonic excitation and steady state behavior the equations of motion can be written in a matrix form as

$$\underbrace{\begin{bmatrix} \mathbf{K} & \mathbf{0} & \mathbf{0} & \dots & \mathbf{0} & \dots & \mathbf{0} \\ \mathbf{0} & \mathbf{H}_{lin,1/1} & \mathbf{0} & \dots & \mathbf{0} & \dots & \mathbf{0} \\ \mathbf{0} & \mathbf{0} & \mathbf{H}_{lin,1/2} & \dots & \mathbf{0} & \dots & \mathbf{0} \\ \vdots & \vdots & \vdots & \ddots & \mathbf{0} & \dots & \mathbf{0} \\ \mathbf{0} & \mathbf{0} & \mathbf{0} & \mathbf{0} & \mathbf{H}_{lin,1/\mu_h} & \dots & \mathbf{0} \\ \vdots & \vdots & \vdots & \vdots & \vdots & \ddots & \mathbf{0} \\ \mathbf{0} & \mathbf{0} & \mathbf{0} & \mathbf{0} & \mathbf{0} & \dots & \mathbf{H}_{lin,v_h/\mu_h} \end{bmatrix}}_{\mathbf{H}_{lin}} \underbrace{\begin{bmatrix} \hat{\mathbf{x}}_0 \\ \hat{\mathbf{x}}_{1/1} \\ \hat{\mathbf{x}}_{1/2} \\ \vdots \\ \hat{\mathbf{x}}_{1/\mu_h} \\ \vdots \\ \hat{\mathbf{x}}_{v_h/\mu_h} \end{bmatrix}}_{\hat{\mathbf{x}}} + \underbrace{\begin{bmatrix} \hat{\mathbf{F}}_{nl,0}(\hat{\mathbf{x}}_0, \hat{\mathbf{x}}_{1/2}, \dots, \hat{\mathbf{x}}_{v_h/\mu_h}) \\ \hat{\mathbf{F}}_{nl,1/1}(\hat{\mathbf{x}}_0, \hat{\mathbf{x}}_{1/2}, \dots, \hat{\mathbf{x}}_{v_h/\mu_h}) \\ \hat{\mathbf{F}}_{nl,1/2}(\hat{\mathbf{x}}_0, \hat{\mathbf{x}}_{1/2}, \dots, \hat{\mathbf{x}}_{v_h/\mu_h}) \\ \vdots \\ \hat{\mathbf{F}}_{nl,1/\mu_h}(\hat{\mathbf{x}}_0, \hat{\mathbf{x}}_{1/2}, \dots, \hat{\mathbf{x}}_{v_h/\mu_h}) \\ \vdots \\ \hat{\mathbf{F}}_{nl,v_h/\mu_h}(\hat{\mathbf{x}}_0, \hat{\mathbf{x}}_{1/2}, \dots, \hat{\mathbf{x}}_{v_h/\mu_h}) \end{bmatrix}}_{\hat{\mathbf{f}}_{nl}(\hat{\mathbf{x}}, \omega)} = \underbrace{\begin{bmatrix} \hat{\mathbf{F}}_{exc,0} \\ \hat{\mathbf{F}}_{exc,1/1} \\ \hat{\mathbf{F}}_{exc,1/2} \\ \vdots \\ \hat{\mathbf{F}}_{exc,1/\mu_h} \\ \vdots \\ \hat{\mathbf{F}}_{exc,v_h/\mu_h} \end{bmatrix}}_{\hat{\mathbf{f}}_{exc}}, \quad (13)$$

$$\text{with } \mathbf{H}_{lin,v_h/\mu_h} = \mathbf{K} + i \left(\frac{v_h}{\mu_h} \omega \right) \mathbf{D} - \left(\frac{v_h}{\mu_h} \omega \right)^2 \mathbf{M}. \quad (14)$$

3.1 Solution Method

The nonlinear system given in Eq. (14) cannot be solved explicitly as the nonlinear forces depend on $\hat{\mathbf{x}}$. Hence, they are transformed in an implicit form such that a residual $\mathbf{r}(\hat{\mathbf{x}}_m, \omega_m)$ can be iterated to zero

$$\mathbf{r}(\hat{\mathbf{x}}, \omega) = \mathbf{H}_{lin} \hat{\mathbf{x}} + \hat{\mathbf{f}}_{nl}(\hat{\mathbf{x}}, \omega) - \hat{\mathbf{f}}_{exc} \stackrel{!}{=} \mathbf{0}. \quad (15)$$

For this task a predictor-corrector method is used including a tangent prediction step

$$\hat{\mathbf{x}}_p = \hat{\mathbf{x}} + \delta \mathbf{v}, \quad (16)$$

where $\hat{\mathbf{x}}$ denotes the previous solution and $\hat{\mathbf{x}}_p$ the predicted point which is calculated along the tangent vector of the solution curve \mathbf{v} by multiplication with the step size factor δ . For the calculation of the actual solution at the new point a corrector step is performed which can be interpreted as a minimization problem of the form [11]

$$\min \{ |\hat{\mathbf{x}} - \hat{\mathbf{x}}_p|; \mathbf{r}(\hat{\mathbf{x}}, \omega) = \mathbf{0} \}. \quad (17)$$

This means that the point on the curve is found which is closest to the predicted value. This minimization problem can be solved iteratively using a Gauss-Newton like method leading to iterations of the following form

$$\begin{bmatrix} \hat{\mathbf{x}}_{m+1} \\ \omega_{m+1} \end{bmatrix} = \begin{bmatrix} \hat{\mathbf{x}}_m \\ \omega_m \end{bmatrix} - \begin{bmatrix} \mathbf{J}(\hat{\mathbf{x}}_m, \omega_m) \\ \mathbf{v}_m^T \end{bmatrix}^{-1} \begin{bmatrix} \mathbf{r}(\hat{\mathbf{x}}_m, \omega_m) \\ 0 \end{bmatrix}. \quad (18)$$

where $\mathbf{J}(\hat{\mathbf{x}}_m, \omega_m)$ denotes the Jacobian matrix of the function $\mathbf{r}(\hat{\mathbf{x}}_m, \omega_m)$ and \mathbf{v}_m the tangent vector at iteration m . This tangent vector is updated at each iteration by

$$\mathbf{v}_{m+1} = \mathbf{v}_m - \begin{bmatrix} \mathbf{J}(\hat{\mathbf{x}}_m, \omega_m) \\ \mathbf{v}_m^T \end{bmatrix}^{-1} \begin{bmatrix} \mathbf{J}(\hat{\mathbf{x}}_m, \omega_m) \mathbf{v}_m \\ 0 \end{bmatrix}. \quad (19)$$

This method provides super-linear convergence properties [12] and is very robust as the predicted values are usually already near the solution. However, a drawback of this method is that the Jacobian matrix of the system has to be calculated at each iteration step. A popular method for calculation of the Jacobian in the context is the finite differences method which is applicable in a very general way to all kinds of nonlinearity. As this method needs numerous evaluations of the function $\mathbf{r}(\hat{\mathbf{x}}_m, \omega_m)$ it is computationally very expensive and restricted to systems with a limited number of DOFs and harmonics. Additionally, the quality of the computed Jacobian matrix is a critical point in the algorithm concerning the robustness. Thus, in the following a more efficient, analytical alternative is proposed for contact as well as cubic nonlinearities. Generally, the Jacobian matrix of the system in Eq. (15) can be written as

$$\mathbf{J}(\hat{\mathbf{x}}_m, \omega_m) = \begin{bmatrix} \frac{\partial \mathbf{r}(\hat{\mathbf{x}}_m, \omega_m)}{\partial \hat{\mathbf{x}}_m} & \frac{\partial \mathbf{r}(\hat{\mathbf{x}}_m, \omega_m)}{\partial \omega_m} \end{bmatrix} \quad (20)$$

$$\text{with } \frac{\partial \mathbf{r}_h(\hat{\mathbf{x}}_m, \omega_m)}{\partial \hat{\mathbf{x}}_m} = \mathbf{K} + i \left(\frac{v_h}{\mu_h} \omega \right) \mathbf{D} - \left(\frac{v_h}{\mu_h} \omega \right)^2 \mathbf{M} + \frac{\partial \mathbf{f}_{nl}}{\partial \hat{\mathbf{x}}_m} \quad (21)$$

$$\text{and } \frac{\partial \mathbf{r}_h(\hat{\mathbf{x}}_m, \omega_m)}{\partial \omega_m} = \left(i \left(\frac{v_h}{\mu_h} \right) \mathbf{D} - 2 \left(\frac{v_h}{\mu_h} \omega \right) \mathbf{M} \right) \hat{\mathbf{x}}_m + \frac{\partial \mathbf{f}_{nl}}{\partial \omega_m} \quad (22)$$

The differentiation of the linear parts of the function can be calculated straightforward. Whereas differentiation of the nonlinear forces is more complex and explained in the next sections in some detail for both nonlinearities regarded in this contribution.

Besides the calculation of the Jacobian matrix, the control of the step size δ for the prediction step is another key factor to achieve both, robustness and reasonable computational cost. In this case the step size is controlled by a desired number of iterations m_{opt} along with a multi-level trial and error method [3]. This approach is advantageous in case of strong and sudden changes in the function [13] such as sharp bends caused by non-smooth nonlinearities.

3.2 Nonlinear Force and Jacobian calculation for clearance nonlinearity

The analytical formulation for the calculation of nonlinear contact forces due to clearance and their contribution to the Jacobian matrix of the systems is based on the method proposed in [14] and briefly reviewed in this section.

For the following calculations of the nonlinear forces the relative displacement u in the coupling element is written as a vector product of the form

$$u(t) = \mathbf{\Gamma}^T \mathbf{U} \quad (23)$$

with $\mathbf{\Gamma}$ representing the sine and cosine terms of a Fourier series like in Eq. (8)

$$\mathbf{\Gamma} = [1, \cos(\omega t), \cos(\frac{1}{2}\omega t), \dots, \cos(\frac{1}{\mu_h}\omega t), \dots, \cos(\frac{V_h}{\mu_h}\omega t), \sin(\omega t), \sin(\frac{1}{2}\omega t), \dots, \sin(\frac{1}{\mu_h}\omega t), \dots, \sin(\frac{V_h}{\mu_h}\omega t)]^T \quad (24)$$

and \mathbf{U} representing the Fourier coefficients of $u(t)$

$$\mathbf{U} = [a_{u,0}, a_{u,1/1}, a_{u,1/2}, \dots, a_{u,1/\mu_h}, \dots, a_{u,V_h/\mu_h}, b_{u,1/1}, b_{u,1/2}, \dots, b_{u,1/\mu_h}, \dots, b_{u,V_h/\mu_h}]^T \quad (25)$$

The nonlinear force due to clearance can be calculated by evaluating the integral in Eq. (11) which leads to a piecewise defined function of the form

$$\mathbf{F}_{clear} = \begin{cases} \frac{2}{\mu_h T} \sum_i \int_{t_{ci}}^{t_{si}} \mathbf{\Gamma}_+ F_{nl}(\dot{u}, u, t) dt & \text{contact} \\ \mathbf{0} & \text{separation,} \end{cases} \quad (26)$$

where i numbers all sections in which contact in the interface occurs. t_{ci} represents the points in time when the contact happens and t_{si} the points times when separation happens within the period of integration $\mu_h T$. The nonlinear force $\hat{\mathbf{F}}_{nl,rel}$ in the interface for the clearance nonlinearity can be represented using the vector notation introduced in Eq. (23) yielding

$$\mathbf{F}_{clear} = \begin{cases} \frac{2}{\mu_h T} \int_{t_{ci}}^{t_{si}} \pm k_0 \mathbf{\Gamma}_+ (\mathbf{\Gamma}^T \mathbf{U} - z_0) dt & \text{contact} \\ \mathbf{0} & \text{separation.} \end{cases} \quad (27)$$

Since the vector \mathbf{U} does not depend on t the nonlinear force can be written as

$$\mathbf{F}_{clear} = \begin{cases} \pm (k_0 \mathbf{W} \mathbf{U} - k_0 \mathbf{w} z_0) & \text{contact} \\ \mathbf{0} & \text{separation} \end{cases} \quad (28)$$

where \mathbf{W} is an $j \times j$ matrix with $j = 2N + 1$, consisting of sine and cosine functions of t

$$\mathbf{W} = \frac{2}{\mu_h T} \sum_i \int_{t_{ci}}^{t_{si}} \mathbf{\Gamma}_+ \mathbf{\Gamma}^T dt. \quad (29)$$

and \mathbf{w} is an $j \times 1$ vector also consisting of sine and cosine functions of t

$$\mathbf{w} = \frac{2}{\mu_h T} \sum_i \int_{t_{ci}}^{t_{si}} \mathbf{\Gamma}_+ dt. \quad (30)$$

This integral can be calculated analytically which reduces the computational effort for the calculation of the nonlinear force to simple evaluations of an $j \times j$ Matrix. For the calculation of the Jacobian matrix the nonlinear force has to be differentiated with respect to \mathbf{U} leading to

$$\frac{\partial \mathbf{F}_{clear}}{\partial \mathbf{U}} = \begin{cases} \pm k_0 \mathbf{W} & \text{contact} \\ \mathbf{0} & \text{separation} \end{cases} \quad (31)$$

meaning that also the calculation of the Jacobian is reduced to a single evaluation of an $j \times j$ matrix. This obviously reduces the computational effort dramatically compared to the finite differences method. Another advantage is that the analytical formulation is very exact compared to finite differences or Discrete Fourier Transform based methods like used by [15]. Therefore, it also increases the quality of the Jacobian matrix and the nonlinear force resulting in remarkably higher robustness of the solution algorithm.

3.3 Nonlinear Force and Jacobian calculation for cubic nonlinearity

In this Section an extension of the previously described method for the analytical calculation of the Jacobian matrix to polynomial nonlinearities is proposed resulting in a slightly more complex formulation. As in the previous Section the nonlinear force $F_{nl}(\dot{u}, u, t)$ can be calculated according to Eq. (11). For the cubic force F_{cub} this leads under application of the vector formulation introduced in Eq. (23) to

$$\mathbf{F}_{cub} = \frac{2}{\mu T} \int_0^{\mu T} \beta \mathbf{\Gamma}_+ (\mathbf{\Gamma}^T \mathbf{U})^3 dt. \quad (32)$$

Analogous to the previous Section it is desired to decompose this integral into terms dependent on t and on u to be able to calculate an analytical transformation matrix from time domain into the frequency domain and vice versa. However, this decomposition is not as straightforward as it was in the case of clearance because the exponent of the polynomial induces cross terms leading to all sorts of combinations of entries of $\mathbf{\Gamma}$ and \mathbf{U} as well as their squares and cubes.

For clarity in the following the entries of the vectors $\mathbf{\Gamma}$ and \mathbf{U} will be numbered and denoted as $\mathbf{\Gamma} = [\Gamma_1, \Gamma_2, \dots, \Gamma_j]^T$ and $\mathbf{U} = [U_1, U_2, \dots, U_j]^T$ with $j = 2N + 1$, where N represents the total number of harmonics taken into account. With this notation a general polynomial of power p of a vector product can be written as multinomial sum in a multi-index notation

$$(\mathbf{\Gamma}^T \mathbf{U})^p = (\Gamma_1 U_1 + \Gamma_2 U_2 + \dots + \Gamma_j U_j)^p = \sum_{k_1+k_2+\dots+k_j=p} \binom{p}{k_1, k_2, \dots, k_j} (\Gamma_1 U_1)^{k_1} (\Gamma_2 U_2)^{k_2} \dots (\Gamma_j U_j)^{k_j}. \quad (33)$$

This multinomial expression contains

$$\eta = \binom{j+p-1}{p} = \binom{2N+p}{p} = \frac{(2N+p)!}{(2N)!p!} \quad (34)$$

summands each one consisting of a factor which can be traced down to $\mathbf{\Gamma}$ and a factor which can be traced down to \mathbf{U} as well as a constant multiplier represented by the binomial coefficient. The multinomial can be decomposed into two vectors $\mathbf{\Gamma}^*$ and \mathbf{U}^* , both of the size $\eta \times 1$, with $\mathbf{\Gamma}^*$ containing all factors coming from $\mathbf{\Gamma}$ combined with the constant multipliers of the binomial coefficient and \mathbf{U}^* including the factors dependent on \mathbf{U} , respectively. This means that as desired $\mathbf{\Gamma}^*$ depends on the time and \mathbf{U}^* on the relative displacement only.

Exemplary this decomposition is demonstrated in the following for the case of a cubic polynomial and one harmonic. In this case the power of the polynomial is $p = 3$ and the length of the example vectors $\mathbf{\Gamma}_{ex}$ and \mathbf{U}_{ex} is $j = 3$ reducing Eq. (35) to

$$\left(\begin{bmatrix} \Gamma_1 \\ \Gamma_2 \\ \Gamma_3 \end{bmatrix}^T \begin{bmatrix} U_1 \\ U_2 \\ U_3 \end{bmatrix} \right)^3 = (\Gamma_1 U_1 + \Gamma_2 U_2 + \Gamma_3 U_3)^3 = \sum_{k_1+k_2+k_3=3} \binom{3}{k_1, k_2, k_3} (\Gamma_1 U_1)^{k_1} (\Gamma_2 U_2)^{k_2} (\Gamma_3 U_3)^{k_3}. \quad (35)$$

Expansion of this multinomial expression yields

$$\begin{aligned} (\mathbf{\Gamma}_{ex}^T \mathbf{U}_{ex})^3 &= \Gamma_1^3 U_1^3 + \Gamma_2^3 U_2^3 + \Gamma_3^3 U_3^3 \\ &+ 3\Gamma_1^2 U_1^2 \Gamma_2 U_2 + 3\Gamma_1^2 U_1^2 \Gamma_3 U_3 + 3\Gamma_1 U_1 \Gamma_2^2 U_2^2 + 3\Gamma_2^2 U_2^2 \Gamma_3 U_3 + 3\Gamma_1 U_1 \Gamma_3^2 U_3^2 + 3\Gamma_2 U_2 \Gamma_3^2 U_3^2 \\ &+ 6\Gamma_1 U_1 \Gamma_2 U_2 \Gamma_3 U_3 \end{aligned} \quad (36)$$

The summands of Eq. (36) can now be decomposed into two vectors $\mathbf{\Gamma}_{ex}^*$ and \mathbf{U}_{ex}^* both of size 10×1 yielding

$$\mathbf{\Gamma}_{ex}^* = [\Gamma_1^3, \Gamma_2^3, \Gamma_3^3, 3\Gamma_1^2 \Gamma_2, 3\Gamma_1^2 \Gamma_3, 3\Gamma_1 \Gamma_2^2, 3\Gamma_2^2 \Gamma_3, 3\Gamma_1 \Gamma_3^2, \Gamma_2 \Gamma_3^2, 6\Gamma_1 \Gamma_2 \Gamma_3]^T \quad (37)$$

which is only dependent on entries of $\mathbf{\Gamma}_{ex}$ combined with constant multipliers and

$$\mathbf{U}_{ex}^* = [U_1^3, U_2^3, U_3^3, U_1^2 U_2, U_1^2 U_3, U_1 U_2^2, U_2^2 U_3, U_1 U_3^2, U_2 U_3^2, U_1 U_2 U_3]^T \quad (38)$$

which only depends on the vector \mathbf{U}_{ex} leading to the desired decomposition of time and displacement dependency. The same method as illustrated in this example for the fundamental harmonic and cubic polynomial is applicable in a very general way according to Eq. (35) for higher and subharmonic ansatz functions as well as for general polynomials of power p .

Using the decomposition of the ansatz for u into vectors the $\mathbf{\Gamma}^*$ and \mathbf{U}^* the cubic force can be written as

$$\mathbf{F}_{cub} = \frac{2}{\mu T} \int_0^{\mu T} \beta \mathbf{\Gamma}_+ \mathbf{\Gamma}^{*T} \mathbf{U}^* dt. \quad (39)$$

Now, analogous to the previous section the integration can be separated from the calculation of the nonlinear force yielding a matrix

$$\mathbf{W}^* = \frac{2}{\mu T} \int_0^{\mu T} \mathbf{\Gamma}_+ \mathbf{\Gamma}^{*T} dt \quad (40)$$

of the size $\eta \times (2N + 1)$ which can be calculated analytically. Using this matrix the nonlinear force can be calculated by evaluation of the equation

$$\mathbf{F}_{cub} = \beta \mathbf{W}^* \mathbf{U}^*. \quad (41)$$

As already shown for the clearance nonlinearity, the contribution of the cubic force to the Jacobian matrix can also be calculated analytically. Therefore, the cubic force has to be differentiated with respect to \mathbf{U} yielding

$$\frac{\partial \mathbf{F}_{cub}}{\partial \mathbf{U}} = \beta \mathbf{W}^* \frac{\partial \mathbf{U}^*}{\partial \mathbf{U}} \quad (42)$$

where the partial derivative $\frac{\partial \mathbf{U}^*}{\partial \mathbf{U}}$ can be calculated analytically. This means that the calculation of the cubic force as well as the calculation of their contribution to the Jacobian matrix is reduced to simple matrix evaluations and multiplications. So the same advantages in terms of speed and accuracy are obtained for the cubic nonlinearity as mentioned in the previous Section. Despite it has to be mentioned that the matrices are of a bigger size than for the clearance nonlinearity.

4 Calculation of Nonlinear Normal Modes and Frequency Energy Plots

The fundamental properties of Nonlinear Normal Modes are subject of numerous publications [5, 16] and thus this paper only briefly reviews some aspects about the calculation method used within this publication. According to Rosenberg [17] the NNMs can be defined as synchronous periodic motion of a conservative system. Referring to this definition the NNMs represent the underlying free response of an undamped system of the form

$$\mathbf{M}\ddot{\mathbf{x}} + \mathbf{K}\mathbf{x} + \mathbf{F}_{nl}(\mathbf{x}, t) = \mathbf{0}. \quad (43)$$

This approach seems restrictive as it is limited to undamped systems. There are also extensions to this basic definition taking nonlinear damping into account [18]. However, even considering the basic definition can be of interest as the dynamics of a moderately damped system often corresponds to the dynamics of the underlying conservative system. Eg. the resonance peaks of lightly damped systems as regarded in this paper follow the backbone curve represented by the FEP of the underlying conservative system quite well. For the calculation of NNMs the previously described method for the calculation of FRFs was adapted. In the following the conservative system is regarded which means that the phase angle remains constant. This reduces the size of the system from $(2N + 1)n$ to $(N + 1)n$ as it is sufficient to either consider a pure sine or cosine ansatz function in Eq. (8), resulting in faster computations than for the FRFs.

The total energy in the system directly corresponds to the amplitude. It can be calculated as a sum of the energies E_n of all masses m_n which can be expressed in the frequency domain as

$$E_n(\hat{x}, \omega) = \frac{1}{2} m_n \left(\sum_{v=1}^{\infty} \sum_{\mu=1}^{\infty} \frac{v}{\mu} \omega \hat{x}_{nv/\mu} \right)^2. \quad (44)$$

For the calculation of FEPs the energy is regarded as a parameter and the corresponding frequency of the NNM is calculated. Besides, the same solution algorithm using the same continuation method is used than for the calculations of FRFs.

An interesting property of this method compared to the shooting methods which are widely used eg. by [6, 19] is the filtering characteristic of the HBM, meaning that not all internal resonances are captured depending on the number of harmonics considered [20]. This leads to the computational advantage that certain tongues of the FEP can be neglected if they are of minor interest to speed up calculations.

5 Numerical Examples

In this Section the functionality of the method is demonstrated by coupling two exemplary substructures, each consisting of a linear 2DOF-oscillator, by a nonlinear coupling element. The first subsection considers the effect of the clearance nonlinearity. The scope of the second subsection is to show some special characteristics of the proposed method, like the filtering of modal interactions, using the example of the cubic coupling element.

5.1 Coupling with clearance nonlinearity

Firstly, the element with clearance nonlinearity is used for coupling of two identical linear substructures of which one is excited harmonically. The setup displayed in Fig. 2 and the parameters are listed in Tab. 5.1.

The clearance in the regarded example is $z_0 = \pm 0.5m$ and the stiffness $k_0 = 1N/m$ leading to a non-smooth

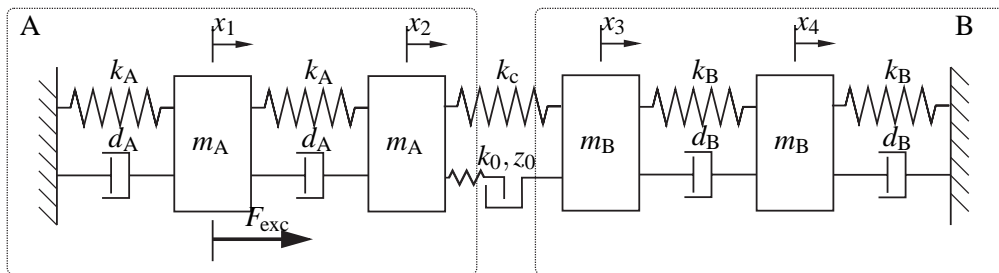


Figure 2: 4 DOF system with clearance coupling element

function for the nonlinear force. To approximate the sudden change in the nonlinear force at the instant the clearance is reached a number of $N = 10$ harmonics is considered for the following calculations.

The FEP of the system is regarded in Fig. 3 to visualize the effect of the coupling with clearance. Therefore,

Parameter	Value	Unit	Parameter	Value	Unit
m_A	1	kg	m_B	1	kg
k_A	1	N/m	k_B	1	N/m
d_A	0.02	Ns/m	d_B	0.02	Ns/m
k_c	0.1	N/m	z_0	± 0.5	m
k_0	1	N/m			

Table 1: Parameters for 4DOF-Oscillator with clearance nonlinearity

the modes of the uncoupled systems (green dots) and the fully coupled system, without clearance (red x) is compared to the coupling with clearance (blue). It is obvious that the clearance induces strong frequency dependence for two of the modes whereas the others remain unchanged. This behavior can be explained by regarding the mode shapes of the fully coupled system which are depicted symbolically in Fig. 3 (left). It can be seen that for the modes 1 and 3 the DOFs 2 and 3 vibrate in unison and there is no nonlinear force

as the relative displacement in the coupling elements is zero, whereas the out of phase modes induce energy dependence due to nonlinearity. Depending on the total energy the behavior of the system can approach the uncoupled or fully coupled system.

On the right side of Fig. 3 the total energy of the forced response for different forcing amplitudes is plotted

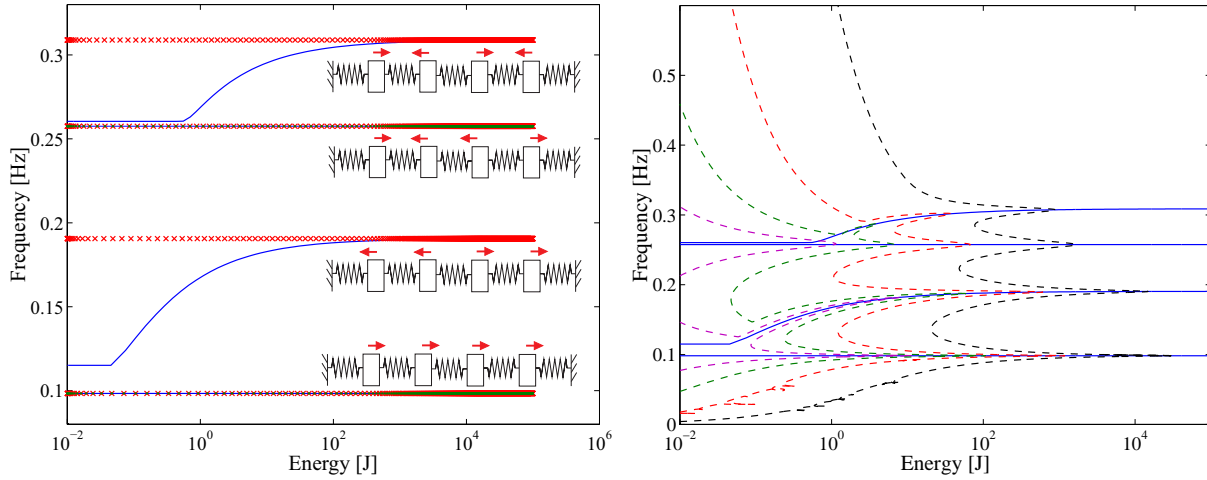


Figure 3: Left: FEP for uncoupled system (green dots), fully coupled system (red x) and system coupled with clearance. Right: FEP and total energy of forced response for excitation with $F_{\text{exc}} = \{0.1, 0.3, 1, 5\} N$.

into the FEP. It can be observed that the peaks of the FRF follow the FEP, which means that the frequency where the peaks are located changes depending on the forcing level. Additionally, several small peaks at lower frequencies are induced by the influence of higher harmonics especially for the high forcing levels.

Fig. 4 shows the receptance of DOF 4 for different forcing amplitudes. For comparison also the FRF for the fully coupled system is plotted. It can be observed that for there is a strong change in the FRF with the changing forcing amplitude leading to bends and multiple solutions. At high forcing level the FRF approaches the linear FRF of the fully coupled system as also shown in the FEPs before. The smaller peaks in the FRF at low frequencies especially for forcing amplitudes of $F_{\text{exc}} = \{1, 5\} N$ are caused by higher harmonics which can be seen in Fig. 4 on the right where the sum of all higher harmonics is depicted for the different forcing levels. For the lower excitation amplitudes $F_{\text{exc}} = \{0.1, 0.3\} N$ there are no such peaks as the contact point is not reached in this low frequency range.

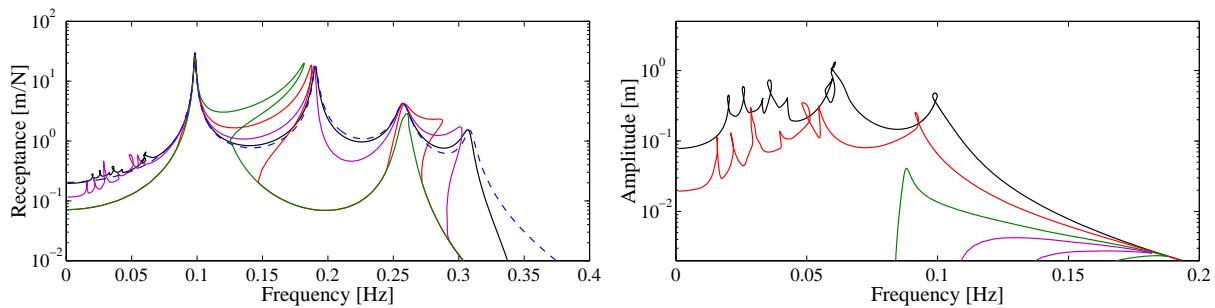


Figure 4: Left: FRF for DOF 4 for excitation with $F_{\text{exc}} = \{0.1, 0.3, 1, 5\} N$ compared with fully coupled system (blue dotted). Right: Sum of higher harmonics for the different forcing amplitudes.

5.2 Coupling with cubic nonlinearity

In the following the cubic spring element representing the automotive bushing is used to couple two different substructures A and B like it is shown in Fig. 5. Each subsystem consists exemplary of a linear 2DOF-

Oscillator. The parameters of the example are listed in Tab. 5.2.

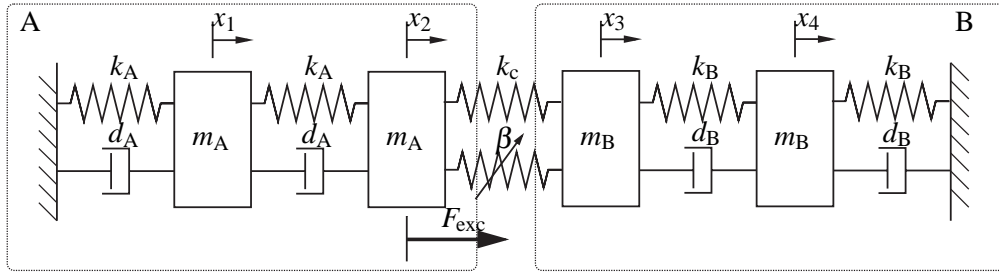


Figure 5: 4 DOF system with cubic coupling element

Parameter	Value	Unit	Parameter	Value	Unit
m_A	1	kg	m_B	1	kg
k_A	2	N/m	k_B	1	N/m
d_A	0.05	Ns/m	d_B	0.05	Ns/m
k_c	0.1	N/m	β	0.5	N/m^3

Table 2: Parameters for 4DOF-Oscillator with cubic nonlinearity

The FEP for this example is calculated, taking into account the harmonics $N = 1 - 5$. Fig. 6 shows the FEP for the coupled system and also the total Energy of the forced response with three different forcing amplitudes. It can be observed the FRF evolves with increasing forcing level along the backbone curve represented by the FEP. Additionally some smaller side peaks in the FRF, especially at low frequencies, appear due to higher harmonics. It is also apparent that all modes are affected by the nonlinear coupling element. A closer look on the first three modes on the right of Fig. 6 reveals several tongues in the FEP which are caused by modal interactions. In this plot also the filtering property of the HBM is shown by comparing the FEP calculated with five harmonics to the fundamental harmonic approximation. As the single frequency sinusoidal approximation cannot represent NNM motions with multiple frequencies the internal resonances cannot be captured. However, apart from the internal resonances the FEP is represented quite exact even for this rough approximation. This demonstrates how details of the FEP can be neglected to speed up the calculations. Any number of harmonics can be chosen finding a suitable trade-off between level of detail and computational efficiency of a numerical analysis. This is particularly interesting in the case of a high modal density and many modal interactions. Still it has to be kept in mind that depending on the ansatz certain modal interactions cannot be captured.

Fig. 7 shows exemplary the evolution of the shape of the second NNM for the points P_1 to P_8 for five harmonics (blue) and for one harmonic (dotted purple). The shape helps to identify the internal resonances as 1 : 3 and 1 : 5 resonances. It can also be seen that not only the FEP is approximated with a single harmonic quite well in a broad energy range but also the shape of the NNM. In contrary near the internal resonances like at P_3 the approximation is not as accurate and for points P_4 and P_7 not even a poor single harmonic approximation can be found.

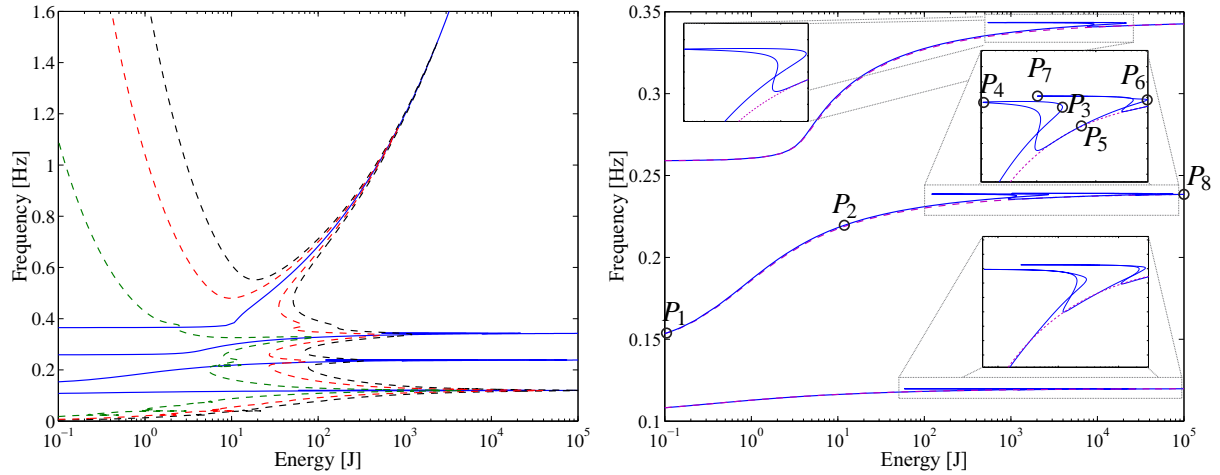


Figure 6: Left: FEP for cubic coupling element with $N=5$ harmonics and total energy of forced response (dotted lines) for excitation with $F_{\text{exc}} = \{3, 9, 18\}N$. Right: Comparison of FEP for the first three modes with 1 (dotted purple) and 5 harmonics with zooms on internal resonances.

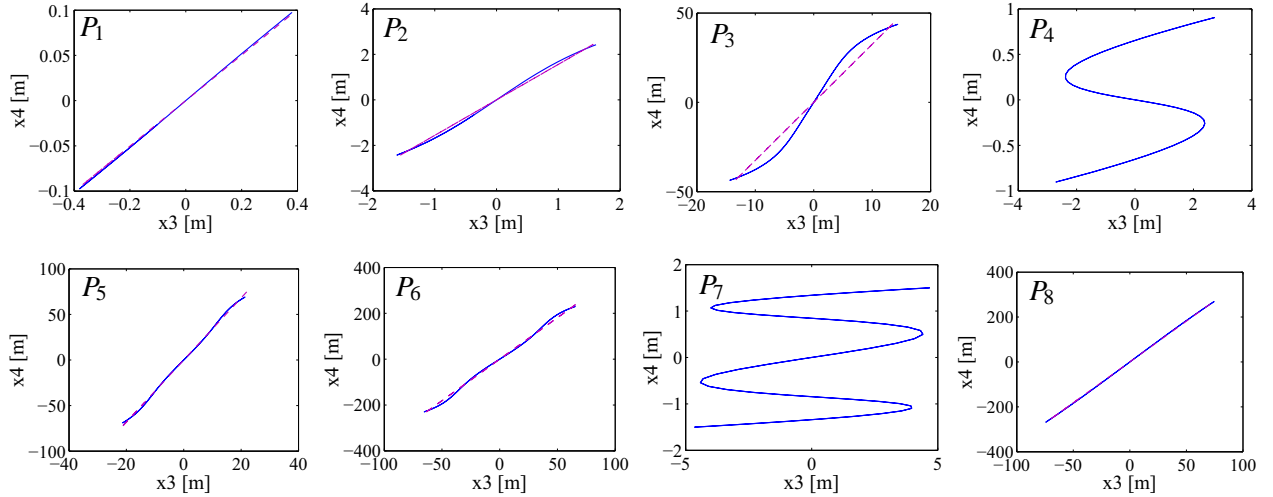


Figure 7: Evolution of NNM shape of mode 2; comparison of fundamental harmonic approximation (dotted purple) and approximation with 5 harmonics (blue)

6 Conclusion and Future Work

This paper presented a method for including nonlinearities in coupled structures by combining substructure formulations with the HBM. Using these methods along with a Continuation Method it is possible to compute FRFs as well as NNMs. The continuation method makes it possible to capture multiple solutions in FRFs and internal resonances in FEPs. For the calculations of the nonlinear forces and the Jacobian matrices, which are necessary for the solution algorithm, analytical formulations were used for the clearance nonlinearity. Additionally, the analytical formulation was extended to polynomial nonlinearities leading to vector formulation for multinomial ansatz functions. The analytical calculation provides the advantage of fast and exact calculations of nonlinear forces and Jacobian matrices. Especially the analytical computation of the Jacobian matrix increases the robustness of the solution algorithm remarkably compared to DFT based methods and the computational efficiency compared to finite differences methods. The simple numerical examples illustrate the effect of coupling with nonlinear elements like energy dependence as well as some properties of the proposed method. For instance the influence of the number of harmonics on the quality of the approximation. In this context also the filtering characteristic of the HBM was demonstrated.

In future the robustness and speed of the calculation method is on the one hand applicable to large scale FE models but on the other hand also new applications are conceivable. For example the use of NNM calculations for nonlinear model updating based on experimental data is within reach. Another future topic could be the extension of the analytical formulations to other nonlinearities like air springs.

References

- [1] Ferreira J.V., (1998), *Dynamic Response Analysis of Structures with Nonlinear Components*, PhD thesis, Imperial College London.
- [2] Schreyer F., Gross J., Reuss P., Junge M., (2014), *Consideration of Interface Damping in Shrouded Mistuned Turbine Blades*, Proceedings of the IMAC-XXXII, Orlando, Florida.
- [3] Peter S., Reuss P., Gaul L., (2014), *Identification of Sub- and Higher Harmonic Vibrations in Vibro-Impact Systems*, Proceedings of the IMAC-XXXII, Orlando, Florida.
- [4] Reuss P., Zeumer B., Herrmann J., Gaul L., (2011), *Consideration of Interface Damping in Dynamic Substructuring*, Proceedings of the IMAC-XXX, Jacksonville, Florida.
- [5] Kerschen G., Peeters M., Golinval J.-C. Vakakis A. F.(2009), *Nonlinear Normal Modes, Part I: A useful framework for the structural dynamicist*, Mechanical Systems and Signal Processing Vol. 23 170-194.
- [6] Peeters M., Vigui R., Srandour G., Kerschen G., Golinval J.-C. (2009), *Nonlinear Normal Modes, Part II: Toward a Practical Computation using Numerical Continuation Techniques*, Mechanical Systems and Signal Processing Vol. 23 195-216.
- [7] De Klerk D., Rixen D., Vormeerens S. (2008), *General Framework for Dynamic Substructuring: History, Review and Classification of Techniques*, AIAA Journal Vol. 46 No. 5 (1169-1181) DOI: 10.2514/1.33274
- [8] Hagedorn P., (1978), *Nichtlineare Schwingungen*, Akademische Verlagsgesellschaft, Wiesbaden.
- [9] Magnus K., Popp K., Sextro W. (2008), *Schwingungen*, Teubner, Wiesbaden
- [10] Nayfeh A.H., Mook D.T. (1979), *Nonlinear Oscillations*, Wiley-Interscience.
- [11] Allgower E.L., Georg K. (1994), *Numerical Path Following*, Department of Mathematics, Colorado State University, Colorado
- [12] Dahmen W., Reusken A., (2008), *Numerik für Ingenieure und Naturwissenschaftler*, Springer, Berlin
- [13] Niet A., (2002), *Step-size control and corrector methods in numerical continuation of ocean circulation and fill-reducing orderings in multilevel ILU methods*, Department of Mathematics, University of Groningen, Groningen
- [14] Petrov E. P., Ewins D. J., (2002), *Analytical Formulation of Friction Interface Elements for Analysis of Nonlinear Multi-Harmonic Vibrations of Bladed Discs*, Proceedings of ASME Turbo Expo 2002, Amsterdam.
- [15] Narayanan S., Sekar P. (1998), *A Frequency Domain based Numeric-Analytical Method for Non-Linear Dynamical Systems*, Journal of Sound and Vibration, Vol. 211 No. 3 (409-424)
- [16] Vakakis A. F., Manevitch L. I., Mikhlin Y. V., Pilipchuk V. N., Zevin A. A. (1996), *Normal Modes and Localization in nonlinear Systems*, John Wiley & Sons Inc, New York.

- [17] Rosenberg R. M. (1960), *Normal modes of nonlinear dual-mode systems*, Journal of Applied Mechanics Vol. 27 263-268.
- [18] Laxalde D., Thouverez F. (2009), *Complex Non-Linear Modal Analysis for Mechanical Systems: Application to Turbomachinery Bladings With Friction Interfaces*, Journal of Sound and Vibration Vol. 322 1009-1025.
- [19] Kuether R. J., Allen M. S. (2014), *A numerical approach to directly compute nonlinear normal modes of geometrically nonlinear finite element models*, Mechanical Systems and Signal Processing Vol. 46 1-15.
- [20] Detroux T., Renson L., Kerschen G., (2014), *The Harmonic Balance Method for Advanced Analysis and Design of Nonlinear Mechanical Systems*, Proceedings of the IMAC-XXXII, Orlando, Florida.